Available online at www.sciencedirect.com
ScienceDirect
Journal of Solid State Chemistry 180 (2007) 1093–1102
JOURNAL OF SOLID STATE CHEMISTRY
www.elsevier.com/locate/jssc

The incommensurately modulated $NiGe_{1-x}P_x$, $\sim 0.3 \leqslant x \leqslant \sim 0.7$, solid solution: The 'missing link' between the *NiP* and *MnP* structure types

A.-K. Larsson[a,*,1], F.J. García-García[b], R.L. Withers[a]

[a]*Research School of Chemistry, Australian National University, Canberra, ACT 0200, Australia*
[b]*Lehrstuhl für Festkörperchemie, Institüt for Physik, Universität Augsburg, Universitätsstrasse 1, D-86159 Augsburg, Germany*

Received 27 September 2006; received in revised form 3 January 2007; accepted 4 January 2007
Available online 14 January 2007

Abstract

The (3 + 1)-d incommensurately modulated structures of four members of the $NiGe_{1-x}P_x$ solid solution field have been successfully refined from X-ray powder diffraction data (R_w(all)/R_{wp} = 2.13/3.92; 1.52/4.25; 1.27/3.44 and 2.00/4.03 for $x = 0.4$, 0.5, 0.6 and 0.7, respectively). The 4-d superspace group symmetry is $Amam(0\,0\,\gamma)s\,0\,0$ ($Z = 4$; $a = 5.0468(2)$, 5.0188(2), 4.9796(2) and 4.9651(1) Å; $b = 6.0636(3)$, 6.0576(2), 6.0183(2) and 6.0031(1) Å; $c = 3.4877(2)$, 3.4812(2), 3.4593(1) and 3.45442(7) Å; $\gamma = 0.7769(2)$, 0.7467(1), 0.7241(1) and 0.7046(1) for $x = 0.4$, 0.5, 0.6 and 0.7, respectively). The underlying average structure is of *NiAs* type while the (in general) incommensurate primary modulation wave-vector, $\gamma\mathbf{c}^*$, varies continuously and smoothly with composition. The two largest amplitude displacive atomic modulation functions (AMFs), for all samples, were the Ni displacement along **b** AMF and the Ge/P displacement along **a** AMF. The refined amplitude of the former was found to systematically increase with P content from 0.215 Å for $NiGe_{0.6}P_{0.4}$ to 0.294 Å for $NiGe_{0.3}P_{0.7}$ while the magnitude of the latter was found to increase with P content from 0.177 Å for $NiGe_{0.6}P_{0.4}$ to 0.253 Å for $NiGe_{0.3}P_{0.7}$. These displacive shifts significantly modulate the local crystal chemistry i.e. the local interatomic distances and co-ordination polyhedra. This continuously variable, incommensurately modulated, intermediate structure type is shown to provide a natural link or bridge between the two extreme end-member structures i.e. NiGe (of *MnP* structure type) and NiP by simply choosing the commensurate options with $\gamma = 1$ and $\frac{1}{2}$ respectively.

Keywords: *NiAs* type structures; *NiP*; *NiGe*; *MnP* type structures; Modulated structures; Powder X-ray diffraction; Ni(Ge/P)

Introduction

The electronic origin of the (commensurate) displacive modulations away from the *NiAs* type average structure (subscript *h* in what follows) that are characteristic of the *MnP* ($\mathbf{a}_{MnP} = \mathbf{a}_h + 2\mathbf{b}_h$, $\mathbf{b}_{MnP} = \mathbf{c}_h$ and $\mathbf{c}_{MnP} = \mathbf{a}_h$) and *NiP* ($\mathbf{a}_{NiP} = \mathbf{a}_h + 2\mathbf{b}_h$, $\mathbf{b}_{NiP} = \mathbf{c}_h$ and $\mathbf{c}_{NiP} = 2\mathbf{a}_h$) structure types (see Fig. 1) have long been of interest to structural chemists [1]. Displacive modulations (in general, incommensurate) away from an underlying *NiAs* structure have also been reported, but not yet structurally characterized, for a $NiGe_{1-x}P_x$, $\sim 0.3 \leqslant x \leqslant \sim 0.7$, solid solution [2]. Clearly, the crystal structure of a general member of this solid solution cannot be described in terms of a commensurate superstructure of the ideal *NiAs* average structure type (as is the case for *MnP* and *NiP* type structures), but must instead be described as an incommensurately modulated structure with a continuously variable, composition-dependent primary modulation wave-vector [2]. In the current paper, emphasis is put upon such a modulation wave approach to describe this incommensurately modulated $NiGe_{1-x}P_x$ solid solution phase as a direct and natural link between the two extreme end-member structures i.e. NiGe (of *MnP* structure type) and NiP.

Vincent and Pretty [3] first detected the incommensurately modulated structure of $NiGe_{1-x}P_x$ and showed that all reflections could be expressed in the form $\mathbf{H} = \mathbf{G} + m\mathbf{q}$,

*Corresponding author. Fax: +61 2 6125 4692.
E-mail address: ankie.larsson@anu.edu.au (A.-K. Larsson).
[1]Formerly at the Research School of Physical Sciences and Engineering, Australian National University.

0022-4596/$ - see front matter © 2007 Elsevier Inc. All rights reserved.
doi:10.1016/j.jssc.2007.01.006

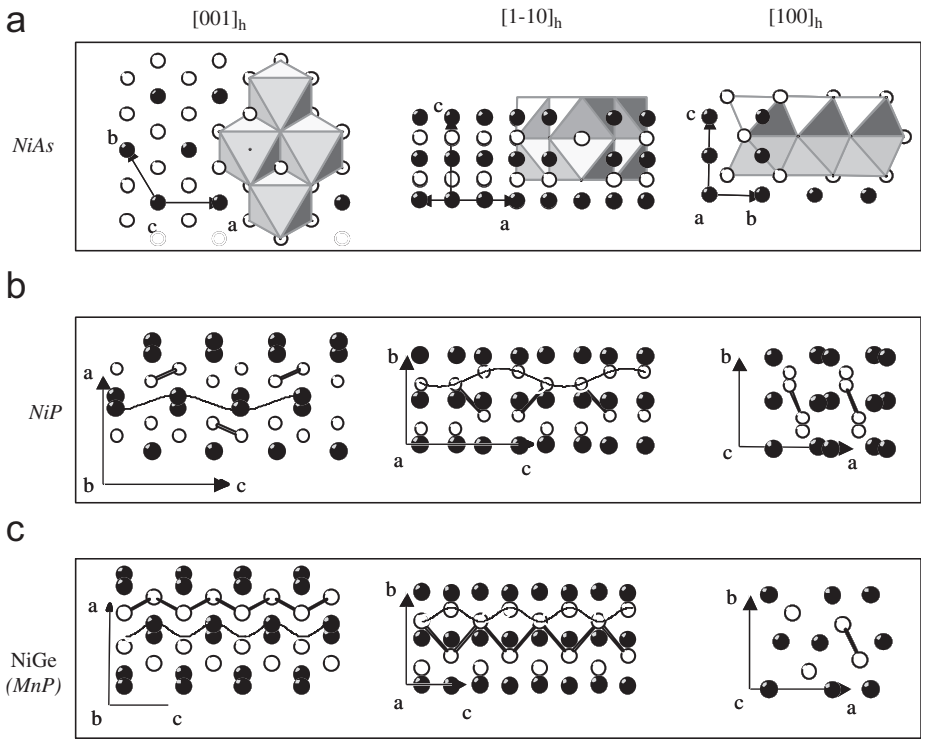

Fig. 1. Shows the (a) NiAs, (b) NiP and (c) NiGe structures projected along the [0 0 1], [1 $\bar{1}$ 0] and [1 0 0] directions of the underlying *NiAs* type structure. Black spheres indicate the transition metal atoms and light spheres indicate the P/Ge/As atoms. The short P–P bonds in NiP (2.42 Å) as well as the medium short Ge–Ge bonds in NiGe (2.78−2.80 Å) are indicated. These bonds greatly distort the underlying octahedra in the substructure (indicated in (a)). The distortions away from the underlying *NiAs* type average structures can be described with modulation waves as indicated with sine waves in (b) and (c).

where **G** represents a Bragg reflection belonging to the underlying *NiAs* type average structure, m is an integer and the primary modulation wave-vector $\mathbf{q} = \gamma_h[1\,1\,0]^*$ with $\gamma_h \approx 0.35$. Shortly thereafter, Withers and Bird [4] used a quantitative fitting procedure to large angle convergent beam electron diffraction patterns to extract precise but limited structural information as to the displacement eigenvectors associated with some of the observed modulation wave-vectors. On the basis of this quantitative fitting, it was concluded that the modulations were "… overwhelmingly displacive rather than compositional in origin…" [4]. Since then, two *NiAs*-related, superstructure phases in the $NiGe_{1-x}P_x$ system have been reported with Ge and P atoms at distinct crystallographic positions: $Ni_5Ge_2P_3$ [5] whose (conventional 3-d) structure was refined from single crystal data and Ni_2GeP [6] whose structure was never refined but assumed to be isostructural to the Ni_2SiP structure type [7] based on a comparison of calculated theoretical powder diffraction intensities with experimental powder patterns.

Our own recent TEM investigation of the $NiGe_{1-x}P_x$ system [2], showed that this $NiGe_{1-x}P_x$ phase has an extended homogeneity range: γ_h was found to be composition-dependent and to vary continuously between ~0.33 (for $x = 0.7$) and ~0.46 (for $x = 0.3$). This strongly suggests that isolated superstructure line phases as such do not exist within this $NiGe_{1-x}P_x$ system. Rather, the system should be described as one continuously variable, incommensurately modulated, solid solution phase. The precise nature of the modulation, however, remained unclear. In this contribution, we report the results of incommensurate structure refinements of this $NiGe_{1-x}P_x$ phase at four different compositions within the solid solution field: namely at $x = 0.4$, 0.5, 0.6 and 0.7. In addition, it is demonstrated how this incommensurately modulated structure of $NiGe_{1-x}P_x$ provides a natural link or bridge between the two extreme end-member structure types i.e. NiGe (of *MnP* structure type) and NiP (of *NiP* structure type). Such a link is totally compatible with the suggested electronically driven origin of the end-member structure types [1].

1. Experimental

1.1. Sample preparation

The four $NiGe_{1-x}P_x$ samples ($x = 0.4$, 0.5, 0.6 and 0.7) used for the collection of X-ray diffraction data are the same as were used in the preceding TEM study [2]. The elements were mixed, sealed in evacuated silica tubes, placed in an oven and heated to 1000 °C with a temperature increment of 100 °C/day. After 7 days, the silver coloured samples were quenched, ground, resealed in silica tubes and then annealed at 800 °C for a further month before the ampoules were water quenched.

The dominant phase present in each case was the desired $NiGe_{1-x}P_x$ phase. A minor phase, $Ni_2Ge_{1-x}P_x$, of Ni_2P structure type ($P\bar{6}2m$, $a = 5.859$ Å and $c = 3.382$ Å, [8]) was found in all four samples (see Table 1) as well a small amount of a Ge and P-rich amorphous phase [2]. In the case of the most Ge-rich $x = 0.4$ sample, a trace amount of a further impurity phase $Ni_{1+x}Ge$ of $Ni_2In-NiAs$ structure type [9,10] was also detected (see Table 1). Despite the presence of these minor impurity phases, EDS spectroscopy confirmed that the composition of the dominant $NiGe_{1-x}P_x$ phase was very close to the nominal stoichiometry in each case (see [2] for the details).

1.2. Data collection

The data was collected on a STOE STADI-P diffractometer in transmission mode using Cu $K\alpha_1$ radiation from a curved Ge(1 1 1) monochromator. Data was collected in the 2θ range $10^\circ-90^\circ$ with a step size of 0.02° and a step time of 400 s. The generator settings were 45 kV and 50 mA.

2. Superspace symmetry, structure refinement and structure description

2.1. Superspace symmetry considerations

The $(3+1)$-d superspace group symmetry of the $NiGe_{1-x}P_x$ solid solution is $Amam(0\,0\,\gamma)s\,0\,0$ (No. 63.6 in Table 9.8.3.5 of [11]) in the standard setting (see [2] for details) whilst the magnitude of the incommensurate primary modulation wave-vector $\gamma = 2\gamma_h \sim 0.78$, 0.75, 0.72 and 0.70 for the $x = 0.4$, 0.5, 0.6 and 0.7 samples, respectively. The relationship between the orthorhombic *Amam* average structure unit cell (standard setting *Cmcm*) and that of the ideal hexagonal *NiAs* parent structure is given by $\mathbf{a} = -\mathbf{c}_h$, $\mathbf{b} = -\mathbf{a}_h + \mathbf{b}_h$ and $\mathbf{c} = \mathbf{a}_h + \mathbf{b}_h$ ($\mathbf{a}^* = -\mathbf{c}_h^*$, $\mathbf{b}^* = \frac{1}{2}[-\mathbf{a}_h^* + \mathbf{b}_h^*]$ and $\mathbf{c}^* = \frac{1}{2}[\mathbf{a}_h^* + \mathbf{b}_h^*]$) with one independent Ni atom (on Wyckoff position 4*a* at 0, 0, 0) and one independent Ge/P atom (at Wyckoff position 4*c* at $\frac{3}{4}$, y, 0, with $y \sim 0.33$). The above superspace group allows Ni displacements along **a** and **b** as well as Ge/P displacements along **a** for odd order harmonics and Ni displacements along **c** as well as Ge/P displacements along **b** and **c** for even order harmonics. It forbids occupational Ge/P ordering for the odd order harmonic modulation waves, in particular for the strongest first order harmonic, strongly suggesting that the driving force for the modulation is displacive rather than occupational in origin.

Apart from the obvious superspace unit cell lattice translation operations, the generators of the above superspace group can be taken to be $\{x_1, x_2 + \frac{1}{2}, x_3 + \frac{1}{2}, x_4\}$, $\{\frac{1}{2} - x_1, x_2, x_3, \frac{1}{2} + x_4\}$, $\{\frac{1}{2} + x_1, -x_2, x_3, x_4\}$ and $\{-x_1, -x_2, -x_3, -x_4 + 2\phi\}$ respectively. The parameter ϕ, the global phase parameter, formally determines the resultant conventional 3-d space group symmetry if γ locks in to an exact rational fraction p/q (see e.g. [12]). Whilst we believe that γ never truly locks into an exact rational fraction, these derived conventional 3-d space group symmetries are nonetheless important when we come to consider the relationship between the $NiGe_{1-x}P_x$ solid solution, the previously published 3-d superstructure refinements within this solid solution field and the extreme end-member NiGe and NiP structures.

The resultant 3-d space group symmetry, for example, is given by *Pcam* if $\phi = 2J/4q$, *Pcab* if $\phi = (2J+1)/4q$ and $Pca2_1$ otherwise if p is odd and q is even (J, p and q all integers)—as is the case for Ni_2GeP ($\gamma = \frac{3}{4}$), $Ni_5Ge_3P_2$ ($\gamma = \frac{7}{10}$) as well as for the hypothetical $x = 1$ end-member compound NiP ($\gamma = \frac{1}{2}$). It is no coincidence that previously published structure refinements for $Ni_5Ge_3P_2$, Ni_2GeP and NiP were carried out in space group *Pbca* (equivalent to *Pcab* in our space group setting). On the other hand, if p and q are both odd, as is the case for the other hypothetical $x = 0$ end-member compound NiGe ($\gamma = \frac{1}{1}$), then the resultant 3-d space group symmetry is given by *Pnab* if $\phi = 2J/4q$, *Pnam* if $\phi = (2J+1)/4q$ and $Pna2_1$ otherwise. Again the reported space group symmetry for NiGe of *Pnma* (*Pnam* in our setting) is one of these allowed resultant 3-d space group symmetries. Thus the whole solid

Table 1
Refined cell parameters, primary modulation wave-vector magnitudes and Ge/P ratios of the $x = 0.4$, 0.5, 0.6 and 0.7 $NiGe_{1-x}P_x$ compositions

Nominal composition	$NiGe_{0.6}P_{0.4}$	$NiGe_{0.5}P_{0.5}$	$NiGe_{0.4}P_{0.6}$	$NiGe_{0.3}P_{0.7}$
$a[NiGe_{1-x}P_x]$	5.0468(2)	5.0188(2)	4.9796(2)	4.9651(1)
$b[NiGe_{1-x}P_x]$	6.0636(3)	6.0576(2)	6.0183(2)	6.0031(1)
$c[NiGe_{1-x}P_x]$	3.4877(2)	3.4812(2)	3.4593(1)	3.45442(7)
$\gamma[NiGe_{1-x}P_x]$	0.7769(2)	0.7467(1)	0.7241(1)	0.7046(1)
$x = o[P]/(o[Ge] + o[P])$	0.398(6)	0.514(8)	0.610(7)	0.688(6)
Mass % of $[NiGe_{1-x}P_x]$	87(5)	91(4)	98(2)	96(1)
$a[Ni_2P]$	5.943(2)	5.9037(8)	5.875(2)	5.871(2)
$c[Ni_2P]$	3.367(2)	3.3834(8)	3.380(2)	3.391(2)
Mass % of $[Ni_2P]$	11(1)	9.3(4)	2.4(8)	4.3(5)
$a[Ni_3Ge_2]$	3.828(2)			
$c[Ni_3Ge_2]$	5.014(4)			
Mass % of $[Ni_3Ge_2]$	2.4(6)			

The refined cell dimensions and mass % of impurity phases are also shown.

solution as well as the extreme end-member NiGe and NiP structures may all be described self-consistently using the same modulation wave approach.

2.2. Refinements

The modulated structure refinement program JANA 2000 [13] was used for all refinements. The background, average structure unit cell dimensions and peak shape were initially refined using le Bail decomposition followed by refinement of the unit cell dimensions of the minor impurity phase/s (see Table 1). The magnitude of the primary modulation wave-vector, γ, was then determined followed by refinement of the fractional co-ordinates and atomic displacement parameters (ADPs) of the one independent Ni atom (Wyckoff position 4*a* at 0, 0, 0) and one independent Ge/P atom (Wyckoff position 4*c* at $\frac{3}{4}$, y, 0, with $y\sim0.33$) per average structure unit cell.

Using only the y fractional co-ordinate for the Ge/P position, the Ge/P ratio on this position and isotropic ADPs for the Ni and Ge/P atoms as refineable structural parameters, the fit to the parent reflections was poor for all $NiGe_{1-x}P_x$ samples (R(all) = 6.5, 9.1, 6.5 and 13.2 for $x = 0.4$, 0.5, 0.6 and 0.7, respectively). The introduction of anharmonic ADPs, however, improved the fit dramatically (R(all) = 2.3, 1.8, 1.6 and 2.5 for $x = 0.4$, 0.5, 0.6 and 0.7, respectively). Fourier maps from these anisotropic refinements showed that the average electron density around the Ge/P position was always noticeably elongated along the **a** direction (indicating a significant amplitude for the x sin 1[Ge/P] displacive modulation wave – see below) while the electron density around the Ni position was likewise noticeably elongated along the **b** direction (indicating a significant amplitude for the y sin 1[Ni] displacive modulation wave).

With this anisotropic average structure as a starting model, the various modulations allowed by the overall superspace group symmetry, beginning with the first order harmonic displacive modulation waves, were then successively introduced and their amplitudes refined in conjunction with the already introduced refineable parameters (see Tables 2 and 3). All four refinements proceeded smoothly and produced very similar results despite the differing primary modulation wave-vector magnitudes, γ. The two largest amplitude displacive modulation waves by far, for all samples, were the first order harmonic, Ni displacement along **b** modulation wave amplitude (y sin 1[Ni]) and the Ge/P displacement along **a** modulation wave amplitude (x sin 1[Ge/P]). The refined amplitude of y sin 1[Ni] was found to systematically increase with P content from 0.0355(9) (≡ 0.215 Å) for $NiGe_{0.6}P_{0.4}$ to 0.0490(5) (≡ 0.294 Å) for $NiGe_{0.3}P_{0.7}$ while the magnitude of x sin 1[Ge/P] was found to increase with P content from 0.035(1) (≡ 0.177 Å) for $NiGe_{0.6}P_{0.4}$ to 0.051(1) (≡ 0.253 Å) for $NiGe_{0.3}P_{0.7}$. The Ni displacement along **a** modulation wave amplitude (x sin 1[Ni]) refined to quite small values in each case, typically an order of magnitude smaller than y sin 1[Ni].

The two symmetry-allowed, first order harmonic, modulated ADPs for the Ni atom (see Table 3) invariably significantly improved the fit to the experimental data, in particular to the first order harmonic satellite reflections (R_w(obs) 1st, for example, decreases from 6.12% to 2.30% for $x = 0.6$, see Table 4). The U_{23} cos 1[Ni] term (corresponding to the tilt of the Ni ADP ellipsoid in the yz plane), in particular, was found to be important at all compositions. The other symmetry allowed U_{13} cos 1[Ni] term, on the other hand, refined to very close to zero values and was barely significant for any of the samples (see

Table 2
Final refined average structure parameters of the $x = 0.4$, 0.5, 0.6 and 0.7 $NiGe_{1-x}P_x$ compositions

Nominal composition	$NiGe_{0.6}P_{0.4}$	$NiGe_{0.5}P_{0.5}$	$NiGe_{0.4}P_{0.6}$	$NiGe_{0.3}P_{0.7}$
x[Ge]	0.75	0.75	0.75	0.75
y[Ge]	0.3306(8)	0.3291(6)	0.3330(7)	0.3268(4)
z[Ge]	0	0	0	0
U_{11}[Ge]	0.045(2)	0.035(2)	0.039(2)	0.032(2)
U_{22}[Ge]	0.008(2)	0.006(2)	0.014(2)	0.009(1)
U_{33}[Ge]	0.005(2)	0.008(2)	0.013(2)	0.009(1)
x[Ni]	0	0	0	0
y[Ni]	0	0	0	0
z[Ni]	0	0	0	0
U_{11}[Ni]	0.013(2)	0.009(1)	0.015(2)	0.0083(9)
U_{22}[Ni]	0.034(3)	0.032(2)	0.035(3)	0.020(1)
U_{33}[Ni]	0.050(4)	0.058(3)	0.051(3)	0.049(2)
U_{12}[Ni]	−0.002(4)	0.000(2)	0.005(3)	−0.002(1)

Table 3
Final refined modulation wave amplitude parameters for the $x = 0.4$, 0.5, 0.6 and 0.7 $NiGe_{1-x}P_x$ compositions

Nominal composition	NiGe	$NiGe_{0.6}P_{0.4}$	$NiGe_{0.5}P_{0.5}$	$NiGe_{0.4}P_{0.6}$	$NiGe_{0.3}P_{0.7}$	NiP
x sin 1[Ni]	0.0050	0.005(2)	0.004(1)	0.004(1)	0.0046(8)	0.0160
y sin 1[Ni]	0.0600	0.0355(9)	0.0424(6)	0.0451(7)	0.0490(4)	0.0786
x sin 1[Ge/P]	−0.0620	−0.035(1)	−0.0416(9)	−0.045(2)	−0.051(1)	−0.1041
U_{13} cos 1[Ni]		−0.005(5)	−0.002(4)	−0.006(4)	0.004(3)	
U_{23} cos 1[Ni]		−0.042(4)	−0.050(3)	−0.052(3)	−0.050(2)	
z sin 2[Ni]	0	−0.014(6)	−0.019(3)	−0.21(4)	−0.022(2)	−0.0422

In addition, the equivalent displacive modulation wave amplitudes extracted from NiP and NiGe by Fourier mode decomposition are listed.

Table 4
Residual details for the final refinements of the structures of the $x = 0.4$, 0.5, 0.6 and 0.7 $NiGe_{1-x}P_x$ compositions

Nominal composition	$NiGe_{0.6}P_{0.4}$	$NiGe_{0.5}P_{0.5}$	$NiGe_{0.4}P_{0.6}$	$NiGe_{0.3}P_{0.7}$
R_{wp}	3.92	4.25	3.44	4.03
Parameters	16	16	16	16
R_w(obs)	1.68 (71 + 50)	1.36 (87 + 32)	1.22 (102 + 14)	1.72 (81 + 36)
R_w(all)	2.13	1.52	1.27	2.00
R_w(obs) main	1.18 (25 + 7)	1.10 (30 + 2)	0.98 (32 + 0)	1.37 (27 + 5)
R_w(all) main	1.24	1.10	0.98	1.38
R_w(obs) 1st	3.01 (23 + 14)	1.96 (30 + 6)	2.30 (33 + 1)	3.43 (27 + 7)
R_w(all) 1st	3.75	2.32	2.42	3.59
R_w(obs) 2nd	2.93 (23 + 29)	3.63 (27 + 24)	1.10 (37 + 13)	3.88 (27 + 24)
R_w(all) 2nd	4.56	4.59	1.17	6.26

The number of reflections is indicated in parentheses (observed + unobserved).

Table 3). Modulated displacement parameters of the Ge/P position were found to be small and were hence not used in the final refinements.

The only strong satellite reflections observed in the experimental profiles were of first order (see Fig. 2(a)). The second order satellite reflections were only just observable and no satellite reflections of third or higher order were observed at all. The only other modulation wave amplitudes considered for refinement are thus the second order harmonic terms. In all refinements, the necessarily mixed occupancy of the 4*c* position was dealt with by putting both Ge and P at this position with all parameters restricted to be the same except the occupancy which was refined but with the sum locked to 1. When the symmetry allowed second order harmonic occupational wave for the Ge/P site, $o\cos 2$[Ge/P], was allowed to vary in the refinements of $NiGe_{0.6}P_{0.4}$, $NiGe_{0.5}P_{0.5}$ and $NiGe_{0.4}P_{0.6}$, it never refined to values significantly larger than zero. In the case of $NiGe_{0.3}P_{0.7}$, it refined to the just significant but rather small value of −0.10(2). Fixing $o\cos 2$[Ge/P] to be zero had very little effect on the fit to the second order satellite reflections. It was hence concluded that no occupational order between P and Ge could be detected and the parameter was fixed to zero for the final refinements.

The symmetry-allowed, second order harmonic, displacive modulation wave amplitudes are $z\sin 2$[Ni], $y\sin 2$[Ge/P] and $z\sin 2$[Ge/P]. Comparative refinement showed that only the first of these could be regarded as significant. A small negative value was obtained with a magnitude that steadily increased from 0.014(6) (≡ 0.049 Å) for $NiGe_{0.6}P_{0.4}$ to 0.022(2) (≡ 0.076 Å) for $NiGe_{0.3}P_{0.7}$. The inclusion of this term had a small effect on the second order satellite reflections and none at all on the first order satellite reflections. In the final refinements, this was the only second order harmonic modulation wave term included (see Table 3). In the final structure refinements, there were therefore nine refineable parameters used to describe the average structure reflections, five to describe the first order harmonic satellite reflections and only one for the second order harmonic satellite reflections. The final models at all four compositions describe the 4-d Fourier maps very well. This is shown for the representative $NiGe_{0.4}P_{0.6}$ sample in Fig. 3.

In summary, the clearly dominant displacive modulations away from the underlying average structure are the first order harmonic displacive modulation waves described by the amplitudes $y\sin 1$[Ni], $x\sin 1$[Ge/P] and $U_{23}\cos 1$[Ni]. The final profile fit together with the difference plot for the $x = 0.7$, $NiGe_{0.3}P_{0.7}$, sample is shown in Fig. 2(b). The final residuals for each composition are listed in Table 4 while the final refined structural parameters are listed in Tables 2 and 3.

2.3. Structure description

To illustrate the real space consequences arising from these displacive modulations, a representative section of the refined structure of $NiGe_{0.3}P_{0.7}$ is shown in projection along (a) [1 0 0] and (b) [0 1 0] in Fig. 4. The appearance of these representative real space regions is very similar for each of the four compositions. The Ni displacement along **b** modulation wave with amplitude $y\sin 1$[Ni] and wavelength $1/\gamma \sim 1.42\mathbf{c}$ is drawn in (a) while the Ge/P displacement along **a** modulation wave with amplitude $x\sin 1$[Ge/P] is drawn in (b). In addition, the short Ge/P–Ge/P distances (< 3.12 Å) are indicated by the thick black lines in both (a) and (b). It is interesting to compare with the equivalent projections for the NiP and NiGe structures shown in the first two projections of Fig. 1(b) and (c), respectively. In the case of NiP, isolated P–P dumbbells (P−P = 2.43 Å; see Fig. 1(b)) are present, whereas in the case of NiGe, continuous … Ge–Ge–Ge … chains along the *c* direction (Ge−Ge = 2.82 Å; see Fig. 1(c)) occur. When γ takes intermediate values, as for the $NiGe_{1-x}P_x$ solid solution field, anion chains with short Ge/P–Ge/P distances also result but with an intermediate chain length. Note how fragments of the … Ge–Ge–Ge … chains of NiGe can be identified, as well as disruptions to the chain,

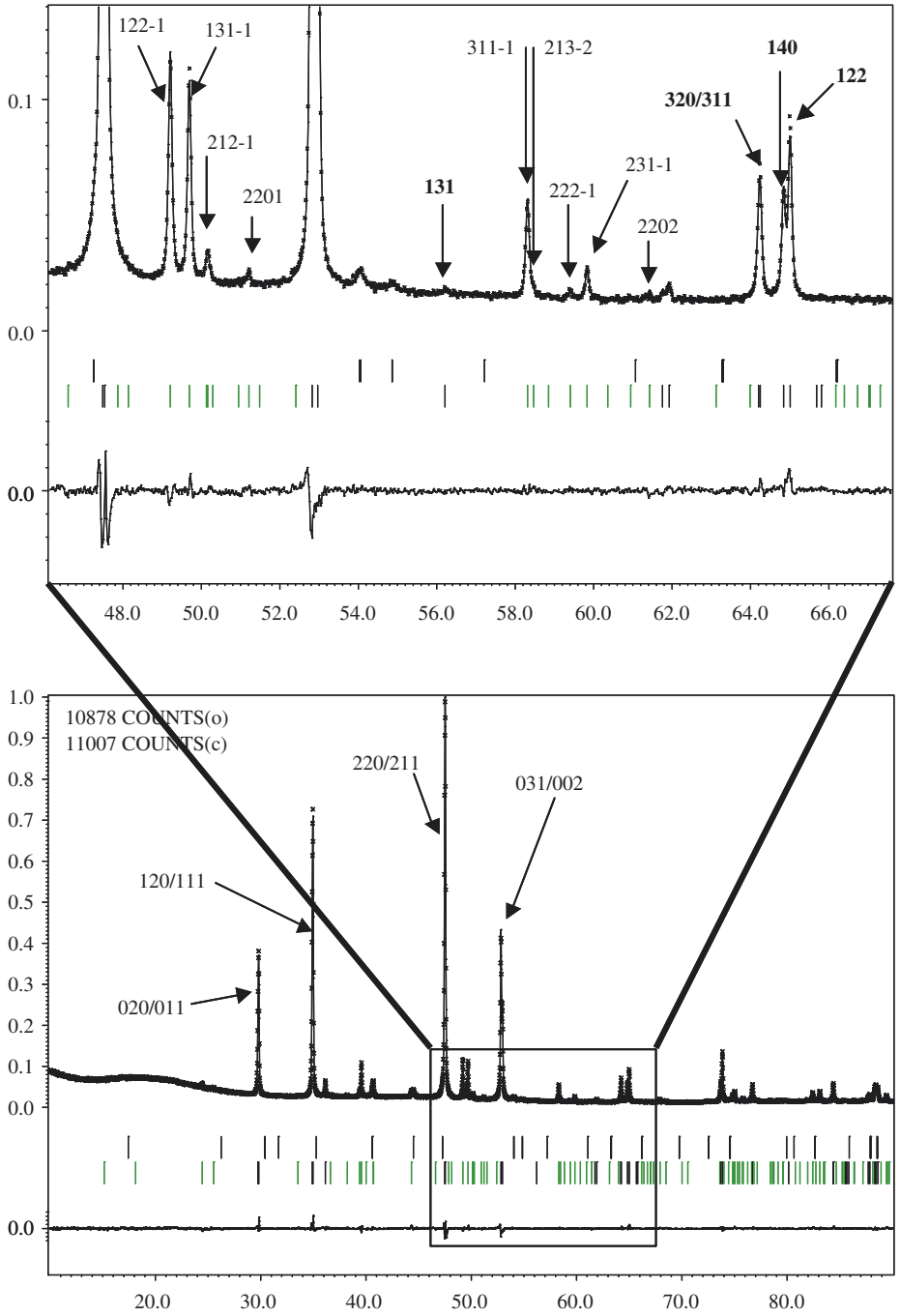

Fig. 2. (a) Shows a blow-up of a portion of the powder profile of the $x = 0.7$, $NiGe_{0.3}P_{0.7}$ sample. The satellite reflections are labelled in 4-index notation. Note that the only strong satellite reflections observed are of first order. (b) Shows the final profile fit for the same $x = 0.7$, $NiGe_{0.3}P_{0.7}$ sample along with the difference profile. The top set of peak markers are for the $Ni_2Ge_{1-x}P_x$ impurity phase while the bottom set of peak markers are for the dominant $NiGe_{0.3}P_{0.7}$ phase.

which can be identified as fragments of the NiP structure, compare Figs. 4(a) and (b) with Figs. 1(b) and (c).

As a result of the refined displacive structural modulations, the Ni–Ni, Ge–Ge and Ni–Ge distances change from one average structure unit cell to the next. Fig. 5 shows the (a) Ni–Ge/P, (b) Ge/P–Ge/P and (c) Ni–Ni distance distributions for the $NiGe_{0.4}P_{0.6}$ sample. The shortest Ge/P–Ge/P separation distance is ~2.88 Å in Fig. 5(b). Given that there are P–P distances as short as 2.43 Å in NiP and Ge–Ge distances as short as 2.82 Å in Ni–Ge, the observed distribution gives no clear indication for preferred locations of Ge and P. As far as the Ni–Ge/P distance distribution goes, in NiGe there is one Ni–Ge distance of 2.330 Å, two of 2.399 Å, two of 2.460 Å and one of 2.487 Å (covering a distance spread ~ one half that apparent in Fig. 5(a)), whereas in NiP there are five Ni–P distances

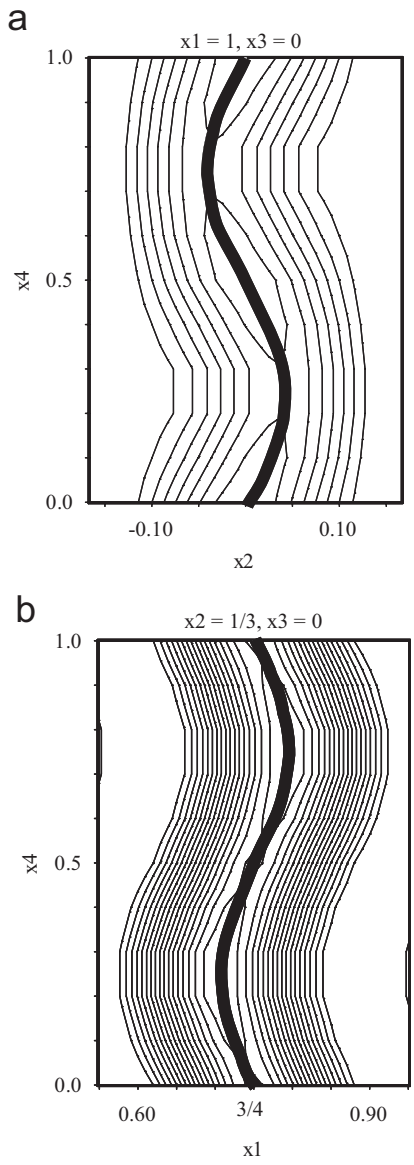

Fig. 3. 2-D cuts through 4-d Fourier maps (for $NiGe_{0.4}P_{0.6}$) demonstrating how well the atomic domains describe the observed electron density. Black thick lines represent Ni in (a) and Ge/P in (b).

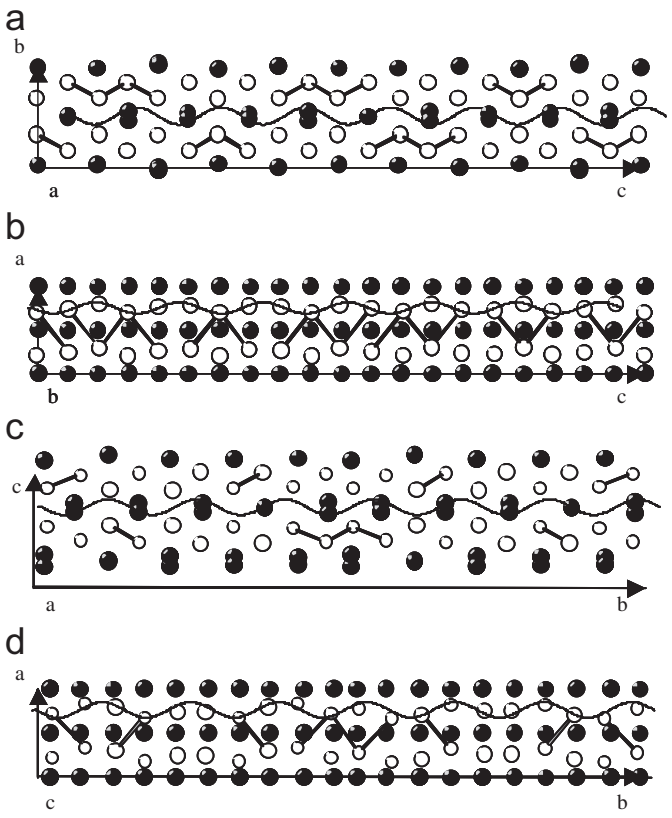

Fig. 4. Projection along (a) [1 0 0] and (b) [0 1 0] of a representative portion of the refined incommensurate structure of $NiGe_{0.3}P_{0.7}$. Ni atoms are drawn as black discs and Ge/P atoms as white discs. Ten subcells along the c direction are shown ($t_0 = \frac{1}{8}$). The Ni displacement along **b** modulation wave with amplitude $y \sin 1[\mathrm{Ni}]$ is shown in (a) while the Ge/P displacement along **a** modulation wave with amplitude $x \sin 1[\mathrm{Ge}]$ is shown in (b). Ge/P–Ge/P distances shorter than 3.12 Å are indicated by thick black lines in both (a) and (b). (c) and (d) Show equivalent projections of the reported crystal structure of $Ni_5Ge_2P_3$. P is indicated with smaller white discs and Ge with larger white discs.

between 2.23 and 2.34 Å and a sixth much longer distance at 2.95 Å. Again there is no clear indication from this for preferred locations for Ge and P in the $NiGe_{1-x}P_x$ structures.

3. Structural relationships

3.1. The relationship to the NiGe and NiP structures

To date, the $NiGe_{1-x}P_x$ solid solution structure type has only been experimentally shown to exist for compositions $\sim 0.3 \leqslant x \leqslant \sim 0.7$ [2]. This does not, however, mean that its composition range might not be able to be extended further towards the extreme end-member compositions of NiGe ($x = 0$) and NiP ($x = 1$) if alternative methods of synthesis are used. Given that these latter two structures can also be described using the same $Amam(0\,0\,\gamma)s\,0\,0$ superspace approach as used for the $NiGe_{1-x}P_x$ solid solution (albeit in a different setting to that normally used), it is intriguing to investigate how close the relationship to the refined structures of the $NiGe_{1-x}P_x$ solid solution really is.

Fig. 6(a) shows the refined a, b and c parameters of the *Amam* average structures as a function of composition all the way from $x = 0$ (NiGe) to $x = 1$ (NiP). For the NiGe structure, the unit cell parameters [14] in the *Pnam* setting are used as the modulation wave-vector magnitude, $\gamma = 1$, preserves the dimensions of the subcell. For NiP, the reported cell parameters [15] in the *Pcab* setting are used except for the fact that the magnitude of $c = \frac{1}{2}c_{\mathrm{NiP}}$ as a result of the fact that $\gamma = \frac{1}{2}$ in this case. Fig. 6(b) shows the relevant γ values as a function of composition. Note that there appears to be, to zeroth order, a systematic linear

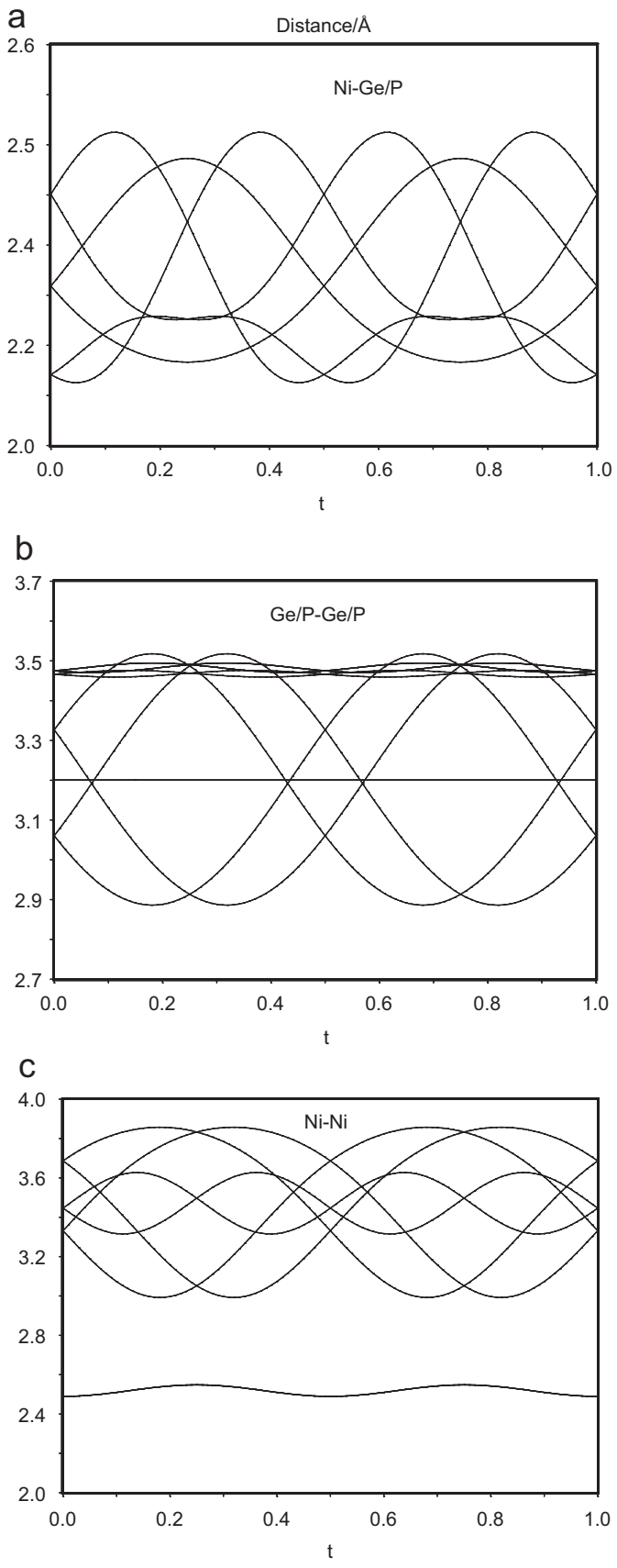

Fig. 5. The Ni–Ni, Ge/P–Ge/P and Ni–Ge/P distance distributions for $NiGe_{0.4}P_{0.6}$ as a function of t. (a) Ni–Ge/P, (b) Ge/P–Ge/P and (c) Ni–Ni.

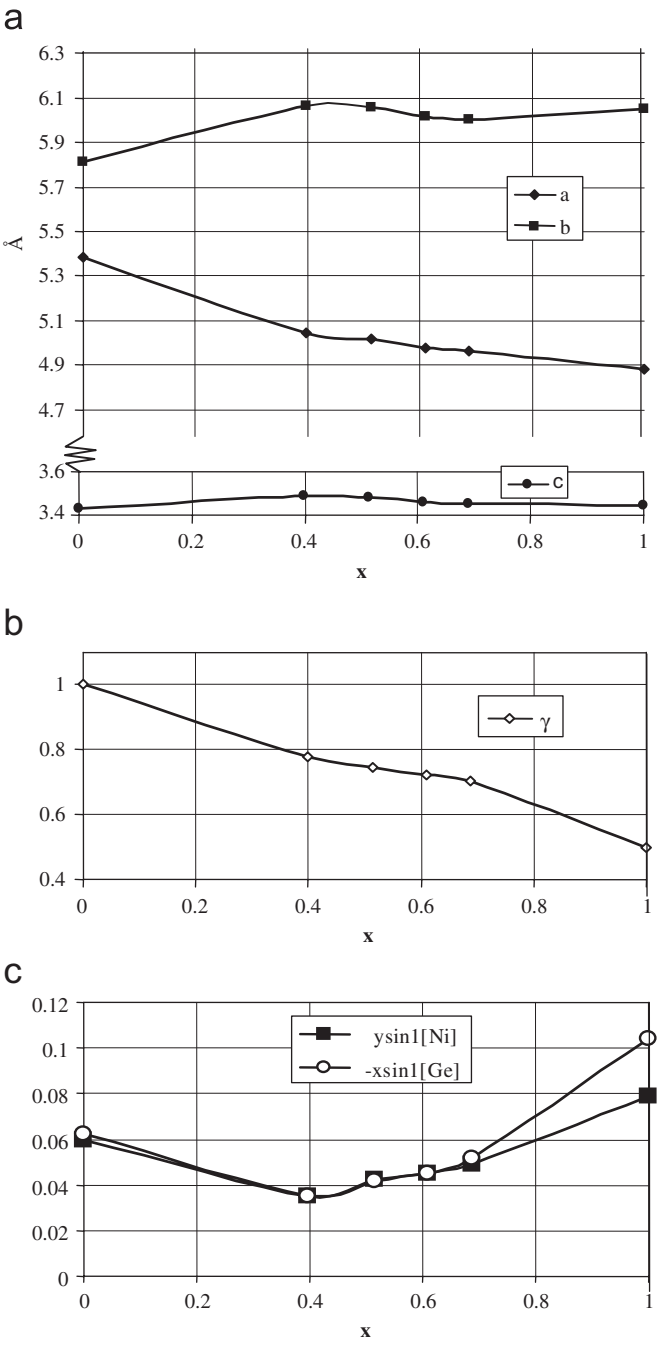

Fig. 6. (a) The a, b and c parameters of the *Amam* average structures, (b) the relevant γ values and (c) the two most important modulation wave amplitudes ($x\sin 1$[Ge/P] and $y\sin 1$[Ni]) plotted as a function of composition from $x = 0$ (NiGe) to $x = 1$ (NiP). The values of x for the ternary samples are taken from the refined occupancies of the Ge/P site.

decrease in the magnitude of γ from the value of 1.0 for $x = 0$ to 0.5 for $x = 1$ that follows the relationship $\gamma = 1 - x/2$. Closer inspection, however, shows that this apparent direct relationship between primary modulation wave-vector magnitude, γ, and composition is not obeyed within the $NiGe_{1-x}P_x$ solid solution region.

These similarities between the modulated structures of $NiGe_{1-x}P_x$ and the hypothetical extreme end-member NiP

and NiGe structure types extend also to the details of their refined crystal structures. As shown in Table 3, by far the dominant modulation wave amplitudes for the $NiGe_{1-x}P_x$ solid solution are y sin 1[Ni] and x sin 1[Ge/P]. The same is also true for NiGe and NiP. Fourier mode decomposition allows the equivalent modulation wave amplitudes to be extracted in the cases of NiP and NiGe (see also Table 3). The refined amplitudes for these two most important modulation waves are also plotted as a function of composition x in Fig. 6(c). Direct extrapolation of the linear trend (within the $NiGe_{1-x}P_x$ solid solution field) for a general increase in the magnitudes of y sin 1[Ni] and x sin 1[Ge/P] with increasing x is consistent with the increased values for these parameters observed for NiP suggesting that the $NiGe_{1-x}P_x$, $0.4 \leqslant x \leqslant 0.7$, solid solution field may actually extend all the way to $x = 1$. In the case of NiGe, on the other hand, the observed values for y sin 1[Ni] and x sin 1[Ge/P] (see Table 3) are significantly larger than might be expected via a simple linear extrapolation of the trend observed within the $NiGe_{1-x}P_x$ solid solution. Likewise, the observed a and b cell parameters for NiGe (see Fig. 6(a)) appear to be significantly different from what might be expected if it were part of the same solid solution field.

3.2. The relationship to the reported $Ni_5Ge_2P_3$ and Ni_2GeP superstructures

As might be expected, the earlier reported superstructure refinements of $Ni_5Ge_2P_3$ [5] and Ni_2GeP [6] from within the $NiGe_{1-x}P_x$ solid solution field also fit very will with the continuously variable, modulated structure approach described in this paper except for the claim of Ge/P ordering in the former. In Fig. 4(c) and (d), for example, the reported structure of $Ni_5Ge_2P_3$ [5] is drawn in projection along (a) [1 0 0] and (b) [0 0 1] for comparison with the equivalent projections of the refined $NiGe_{0.3}P_{0.7}$ structure shown in Fig. 4(a) and (b). To all intents and purposes the structures are identical except for the absence of Ge/P ordering in the latter. The displacive shifts of the Ni and Ge/P atoms in the two superstructures ($Ni_5Ge_2P_3$ and Ni_2GeP) are very well described by the y sin 1[Ni] and x sin 1[Ge/P] modulation wave amplitudes corresponding to the $x = 0.7$ and 0.5 compositions with $\gamma \sim 0.70$ and 0.75, respectively. The reported superstructures are thus commensurate approximant special cases within the one continuously variable $NiGe_{1-x}P_x$ solid solution field.

In the crystal structure report for $Ni_5Ge_2P_3$ [5], the Ge and P atoms are described as being distinct and fully ordered with no statistical mixed distributions. The crystal structure for Ni_2GeP, however, was never refined, but only assumed via a comparison with the reported structure of Ni_2SiP. Our $NiGe_{0.5}P_{0.5}$ sample has both the composition and refined primary modulation wave-vector, $\gamma = 0.7467(2)$, exactly compatible with the published data for Ni_2GeP. Absolutely no tendency for occupancy modulation of the Ge/P site, however, could be detected at this composition. It is therefore inferred that Ge and P are statistically distributed on the same crystallographic site. In the superstructure refinement of $Ni_5Ge_2P_3$, the Ge and P atoms were also reported to be ordered, with three pure P sites and two pure Ge sites. Although the reported composition of $Ni_5Ge_2P_3$ is compatible with the composition of the $NiGe_{0.4}P_{0.6}$ sample, the refined modulation wave-vector of our $NiGe_{0.3}P_{0.7}$ sample is rather closer to 0.70, a prerequisite for the phases to be identical. We therefore assume that our $NiGe_{0.3}P_{0.7}$ sample with the refined composition $NiGe_{0.31}P_{0.69}$ is the closest to the published $Ni_5Ge_2P_3$ phase. Refinement of the $x = 0.4$, 0.5 and 0.6 $NiGe_{1-x}P_x$ samples (see above) showed absolutely no indication for occupational ordering of the Ge/P site. For $x = 0.7$, a barely significant tendency towards occupational ordering was detected. We assume that this tendency was picked up in the single crystal refinement of $Ni_5Ge_2P_3$ [5] which reported a fully Ge/P ordered superstructure phase at this composition.

4. Conclusions

Our refinement results strongly suggest that the $x = 0.4$, 0.5, 0.6 and 0.7 samples are part of the one continuous $NiGe_{1-x}P_x$ solid solution field (see Fig. 6). Even though the currently known homogeneity range for the $NiGe_{1-x}P_x$ phase does not extend as far as the "hypothetical end-members" NiP and NiGe, it turns out that their structures can be very well described using the same displacive modulation waves as occur for the modulated solid solution region. While symmetry allows a direct link between the two extreme end-member structure types i.e. NiGe (of *MnP* structure type) and NiP (of *NiP* structure type), the refined modulation wave amplitudes only support such a link at the high x, NiP, end. While the magnitude of the primary modulation wave-vector for $NiGe_{1-x}P_x$ is a function of the Ge/P ratio, it seems that the driving force for this change may be electronic in origin rather than being directly determined by Ge/P ordering.

Acknowledgment

Financial support from the Swedish Research Council (AKL and JGG) and from the Australian Research Council (AKL and RLW) is gratefully acknowledged.

References

[1] W. Tremel, R. Hoffman, J. Silvestre, J. Am. Chem. Soc. 108 (1986) 5174–5187.
[2] F.J. Garcia-Garcia, A.-K. Larsson, J. Solid State Chem. 178 (2005) 742–754.
[3] R. Vincent, S.F. Pretty, Philos. Mag. A 53 (1986) 843–862.
[4] R.L. Withers, D.M. Bird, J. Phys. C 19 (1986) 3507–3516.
[5] S.V. Orishchin, Y.B. Kuz'ma, Inorg. Mater. 31 (1995) 391–393.
[6] O.N. Il'nitskaya, Y.B. Kuz'ma, Russian J. Inorg. Chem. 35 (1990) 1104–1105.

[7] O.N. Il'nitskaya, Y.B. Kuz'ma, V.S. Fundamenskii, Dopov. Akad. Nauk Ukr. RSR Ser. A 9 (1989) 79–81.
[8] S. Rundqvist, Acta Chem. Scand. 16 (1962) 992–998.
[9] T.P. Agalakova, V.L. Zagryzhskii, P.V. Gel'd, Inorg. Mater. 9 (1973) 1048–1051.
[10] M. Ellner, T. Goedecke, K. Schubert, J. Less-Common Met. 24 (1971) 23–40.
[11] T. Janssen, A. Janner, A. Looijenga-Vos, P.M. de Wolff, Incommensurate and commensurate modulated structures, in: A.J.C. Wilson (Ed.), International Tables for Crystallography, vol. C, Kluwer Academic Publishers, Dordrecht, 1995, pp. 797–835.
[12] J.M. Pérez-Mato, in: J.M. Pérez-Mato, F.J. Zuniga, G. Madariaga (Eds.), Methods of Structural Analysis of Modulated Structures and Quasicrystals, World Scientific, Singapore, 1991, pp. 117–218.
[13] V. Petricek, M. Dusek, L. Palatinus, JANA2000. Vol. Institute of Physics, Praha, Czech Republic, 2000.
[14] H. Pfisterer, K. Schubert, Z. Metallk. 41 (1950) 358–367.
[15] E. Larsson, Arkiv. Kemi. 23 (1965) 335–365.